

Chapter 1

Signal formation in diamond

This chapter describes the fundamentals of signal formation in a diamond sensor, as well as its use as a particle detector. This is described in section ?? where the energy deposition principles are explained. Then examples of ionisation are shown. Later the internal lattice defects that affect the signal are described. The final section contains the description of the remaining part of the signal chain – signal amplifiers, digitisers and devices for signal processing. Noise contributions are discussed at every stage of the signal chain.

Ionisation is the main signal generation mechanism in diamond, silicon and other semiconducting materials. A semiconductor sensor converts the energy deposited by an incident energetic charged particle to an electrical signal. In particular, the particle ionises the atoms in the lattice, freeing electrons and holes, which then drift towards positively and negatively charged electrodes due to an externally applied electrical field, inducing an electrical signal on the electrodes.

Silicon is currently considered as the industry standard for particle detection. However, there are several disadvantages of using silicon instead of diamond, due to significant differences in the material properties. In particular, the properties of silicon change significantly with radiation. For instance, the leakage current increases, which in turn increases shot noise and can lead to a thermal runaway. In addition, due to induced lattice defects, which act as charge traps, its charge collection efficiency is decreased. Both are true for diamond as well, but on a much smaller scale.

Table ?? compares the properties of diamond and silicon. Some of these values are revisited and used in the course of this thesis.

Property	Diamond	Silicon
Band gap energy E_g (eV)	5.5	1.12
Electron mobility μ_e ($\text{cm}^2 \text{V}^{-1} \text{s}^{-1}$)	1800	1350
Hole mobility μ_h ($\text{cm}^2 \text{V}^{-1} \text{s}^{-1}$)	1200	450
Breakdown field (V cm^{-1})	10^7	3×10^5
Resistivity ($\Omega \text{ cm}$)	$> 10^{11}$	2.3×10^5
Intrinsic carrier density (cm^{-3})	$< 10^3$	1.5×10^{10}
Mass density (g cm^{-3})	3.52	2.33
Atomic charge	6	14
Dielectric constant ϵ	5.7	11.9
Displacement energy (eV/atom)	43	13 – 20
Energy to create an e-h pair (eV)	13	3.6
Radiation length (cm)	12.2	9.6
Avg. signal created/ μm (e)	36	89

Table 1.1: Comparison diamond – silicon [?, ?].

1.1 Principles of signal formation in semiconductors

Particles can interact with the sensor in several ways, e.g. via bremsstrahlung [], elastic or inelastic scattering (e-h pair production) or nuclear reactions. Bremsstrahlung is radiation created when a particle is deflected from its original path due to attraction of the core of an atom. This is in principle an unwanted effect in semiconductors as it deteriorate the spatial resolution of the sensor. Elastic scattering is deflection of the particle's trajectory due to the pull from the nucleus without depositing any energy in it. Inelastic scattering is the interaction through which an atom is ionised and an electron-hole pair is created. All these effects are competing and are dependent on the particle's mass, momentum etc.

Semiconductors are materials with a conductance between that of insulators and that of metals – of the order of $10^{25} \Omega^{-1} \text{cm}^{-1}$. They can be made up of atoms with four electrons in their valence band (e.g. silicon–Si, carbon–C or germanium–Ge) or as combinations of two or more different materials (e.g. gallium arsenide–GaAs). The atoms in the lattice form valence bonds with adjacent atoms, making solid crystal structures. These bonds can break apart if sufficient external energy is deposited. The electron that was forming the bond is kicked out, leaving behind a positively charged ion with a vacancy – a hole – in its valence band, as shown in figure ???. A free electron-hole pair is thus created. The free electron travels through the crystal until it is recombined with another hole. Similarly, the hole also “travels” through the material. Its positive charge attracts a bound electron in the vicinity, which breaks from the current bond and moves to the vacancy, leaving a new hole behind. The process continues, making it look like the hole is traveling through the material.

The electrons need to absorb a certain energy to get to get ionised. The minimal transferred energy required to excite an electron in a semiconductor is equal to the energy gap E_g . Typical widths of the forbidden gap are 0.7 eV in Ge, 1.12 eV in Si,

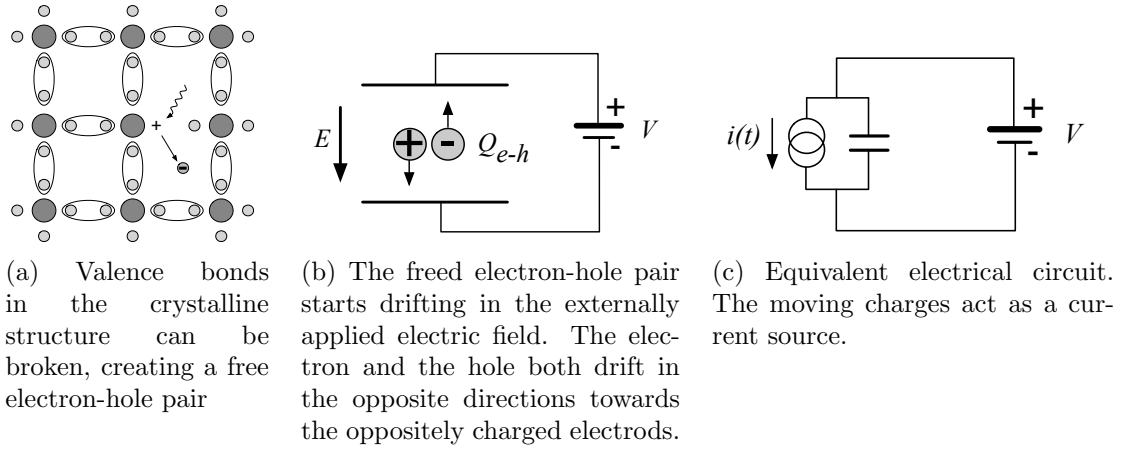


Figure 1.1: In the equivalent electrical circuit diagram the electron-hole creation and drift can be modelled as a current source with a capacitor in parallel.

1.4 eV in GaAs and 5.5 eV in diamond. Due to the small band gap in semiconductors a significant amount of electrons already occupies the conduction band at room temperature (RT) due to thermal excitation, according to the probabilistic distribution. The intrinsic carrier concentration n_i in semiconductors is given as

$$n_i = T^{3/2} \cdot \exp\left(-\frac{E_g}{2k_B T}\right) \quad (1.1)$$

wherein $k_B = 1.381 \times 10^{-23} \text{ m}^2 \text{ kg s}^{-2} \text{ K}^{-1}$ is the Boltzmann constant and T is the temperature in K.

If an external electric field is applied to the crystalline structure, the free electrons and holes drift toward the positive and negative potential, respectively, as shown in figure ???. While drifting, the charges couple with the electrodes, inducing current in the circuit, which is explained by the Shockley–Ramo theorem (see subsection below). The charges recombine upon reaching the electrodes. The equivalent electrical circuit is shown in figure ??.

Energy deposition of α radiation and heavy ions

Energy deposition of β and γ radiation The mean energy loss of a particle traversing the detector with respect to its momentum is given with the the Bethe-Bloch equation []:

$$-\left\langle \frac{dE}{dx} \right\rangle = \frac{4\pi}{m_e c^2} \cdot \frac{nz^2}{\beta^2} \cdot \left(\frac{e^2}{4\pi\epsilon_0} \right)^2 \cdot \left[\ln \left(\frac{2m_e c^2 \beta^2}{I \cdot (1 - \beta^2)} \right) - \beta^2 \right] \quad (1.2)$$

The resulting function for a muon (a heavy electron) is shown in figure ???. At the momentum of around 300 MeV/c the particle deposits the lowest amount of energy. That is called a minimum ionising particle or a MIP.

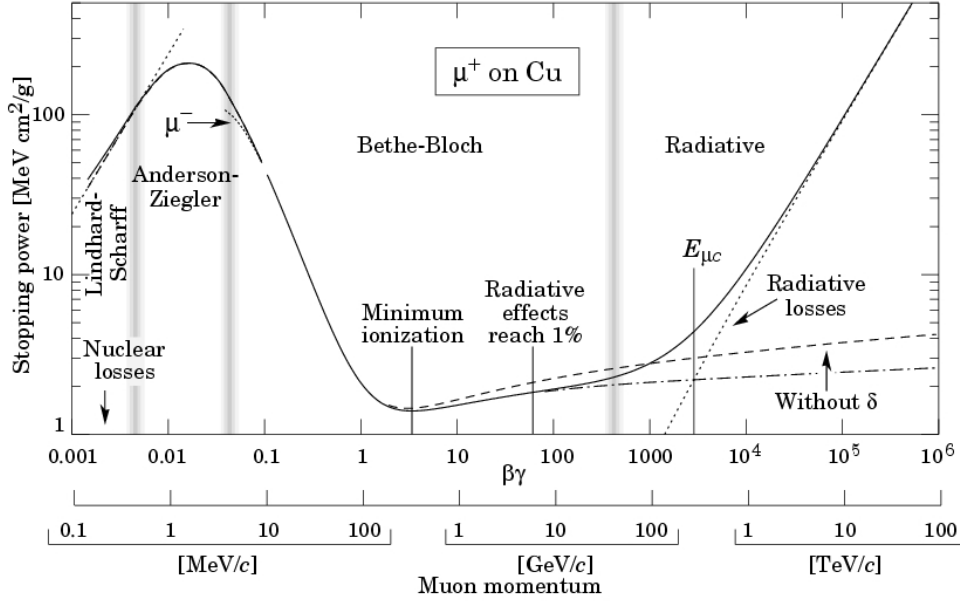


Figure 1.2: Stopping power for muons according to the Bethe-Bloch formula [1].

1.1.1 Signal induction by moving charges

The book [?] gives a simple introduction to understanding signal induction in a conducting plane by a point-like charge. The idea behind it lies in the coupling of the charge with the electrode. The electrode can be in this case modelled as an infinite conducting plane. When the point charge q is created (e.g. an electron-hole pair created via ionisation), its electrostatic field lines immediately couple with the electrode, as seen in figure ?? . The electric field on the metal surface due to a point-like charge q at the distance z_0 equals

$$E_z(x, y) = \frac{qz_0}{2\pi\epsilon_0(x^2 + y^2 + z_0^2)^{\frac{3}{2}}} \quad E_y = E_x = 0. \quad (1.3)$$

A mirror charge appears on the conducting plane, with a charge density distribution

$$\sigma(x, y) = \epsilon_0 E_z(x, y) = \frac{qz_0}{2\pi(x^2 + y^2 + z_0^2)^{\frac{3}{2}}}. \quad (1.4)$$

The charge density integrated over the whole plane gives the mirror charge Q , which has the opposite value of the point charge q :

$$Q = \int_{-\infty}^{\infty} \int_{-\infty}^{\infty} \sigma(x, y) dx dy = -q. \quad (1.5)$$

Now we segment the plane into infinitely long strips with a width w whereby each of the strips is grounded (figure ??). With the charge density distribution ??, the

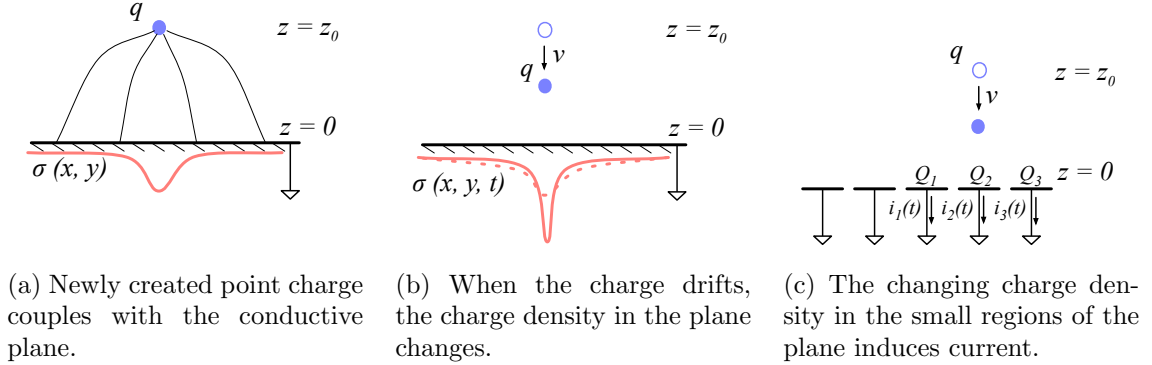


Figure 1.3: A point-like charge inducing current in a conductive plane.

86 resulting mirror charge on a single strip Q_2 directly below the point charge ($x =$
87 $0, y = 0$) reads

$$Q_2(z_0) = \int_{-\infty}^{\infty} \int_{-w/2}^{w/2} \sigma(x, y) dx dy = -\frac{2q}{\pi} \arctan\left(\frac{w}{2z_0}\right) \quad (1.6)$$

88 If the charge starts moving towards the conducting plane, the mirror charge density
89 distribution also changes (see figure ??). This results in the $Q_2[z_0(t)]$ to change with
90 time, inducing an electric current $i_n(t)$:

$$i_n(t) = -\frac{d}{dt} Q_2[z_0(t)] = -\frac{\partial Q_2[z_0(t)]}{\partial z_0} \frac{\partial z_0(t)}{\partial t} = \frac{4qw}{\pi[4z_0(t)^2 + w^2]} v. \quad (1.7)$$

91 The movement of the point-like charge therefore induces current in the conducting
92 plane. The induced current is linearly dependent on the velocity of the point-like
93 charge.

94 W. Shockley [?] and S. Ramo [?] independently proposed a theory which explains
95 how a moving point charge induces current in a conductor. The Shockley-Ramo
96 theorem can therefore be used to calculate the instantaneous electric current induced
97 by the charge carrier or a group of charge carriers. It can be used for any number of
98 electrodes. It states that the current $I_n^{\text{ind}}(t)$ induced on the grounded electrode n by
99 a point charge q moving along a trajectory $\mathbf{x}(t)$ equals

$$I_n^{\text{ind}}(t) = -\frac{dQ_n(t)}{dt} = -\frac{q}{V_w} \nabla \Psi_n[\mathbf{x}(t)] v(t) = -\frac{q}{V_w} E_n[\mathbf{x}(t)] v(t), \quad (1.8)$$

100 where $\mathbf{E}_n(\mathbf{x})$ is the electric field in the case where the charge q is removed, electrode n
101 is set to voltage $V_w = 1$ and all other electrodes are grounded. $\mathbf{E}_n(\mathbf{x})$ is also called the
102 *weighting field* of electrode n and is defined as the spatial differential of the *weighting*
103 *potential*: $\mathbf{E}_n(\mathbf{x}) = \nabla \Psi_n(\mathbf{x})$. In the case of two parallel electrodes, the weighting field
104 is $E_w = -\frac{d\Psi}{dx} = -1/d$, where d is the distance between the electrodes. The resulting
105 induced current is therefore

$$i(t) = \frac{q}{d} v_{\text{drift}}(x, t), \quad (1.9)$$

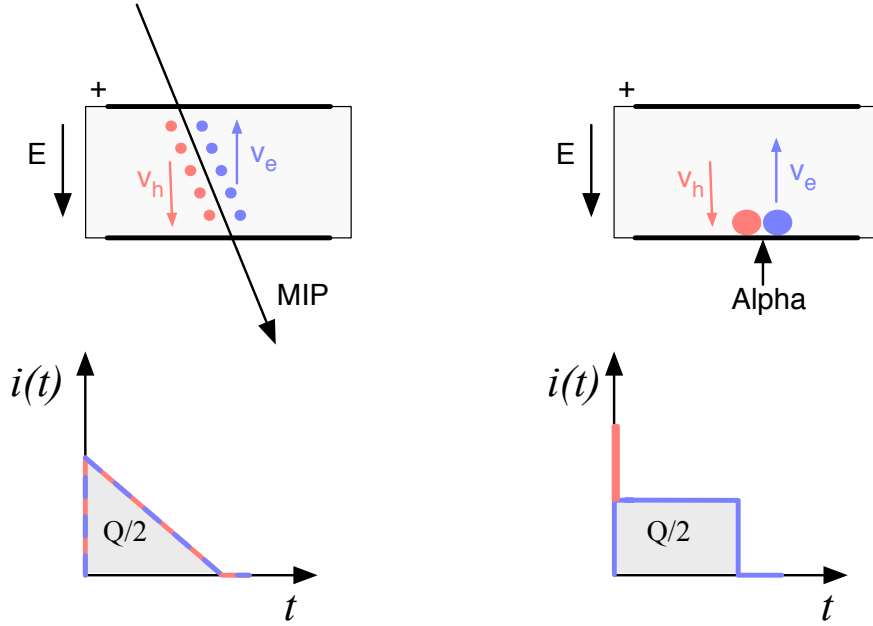


Figure 1.4: Charge carrier drift in diamond for β/γ and for α particles.

106 whereby v_{drift} is the drift velocity of the point-like charge and d is the distance between
107 the electrodes.

1.1.2 Radiation-induced electrical pulses

109 When a highly-energetic particle travels through the sensor, it interacts with atoms
110 in the lattice. It ionises the valence electrons, creating electron-hole (e-h) pairs on its
111 way. It can either deposit only a fraction of its energy and fly exit the sensor on the
112 other side or it can get stopped in the bulk, depositing all of its energy. A special
113 case is when it interacts with the core of the atom in the middle of the sensor via
114 a nuclear interaction. All these various types interactions produce different amounts
115 and different spatial distributions of e-h pairs. The induced electrical current there-
116 fore differs for different types of interaction. Two most frequent types are shown in
117 figure ???. The first diagram shows the interaction of a minimum ionising particle (an
118 electron or a proton) or in some cases a photon, if it is energetic enough. The elec-
119 trons and holes are created all along the trajectory of the particle and immediately
120 start drifting towards the positive and negative electrode, respectively. At the be-
121 ginning, all charges drift and contribute to the induced current. Those closest to the
122 electrodes have a very short drift path and recombine quickly, reducing the induced
123 current. Gradually all the charge carriers recombine. The resulting current signal is
124 a triangular pulse with a sharp rising edge and a linear falling edge. The accumu-
125 lated charge Q_s equals to the sum of the contributions of the positive and negative

charge carriers. The second type of interaction happens when the particle is stopped in the diamond close to the point of entry. Most of its energy is deposited in a small volume close to the electrode. A cloud of charge carriers is created and the charges with the shorter path to the electrode recombine almost instantly. The carriers of the opposite charge, however, start drifting through the sensor to the other electrode. In an ideal diamond sensor, their velocity is constant throughout the drift up until they recombine on the other side. The contribution of the first charge cloud is a peak with a short time. The cloud drifting through the sensor, on the other hand, induces a current signal with a flat top. The resulting signal has a shape of a rectangle, with a spike in the beginning. This spike is filtered out in a real device because it is too fast for the electronics existing currently. The accumulated charge Q_s is equal to a half of the deposited charge by the stopped particle.

The two aforementioned types of interactions have well defined signal responses. Nuclear interactions on the other hand yield various results. The resulting signal shape depends on the decay products of the interaction – they can be α , β or γ quanta, inducing a mixed shaped signal.

1.1.3 Signal charge fluctuations

Two of the important sensor characteristics are the magnitude of the signal and the fluctuations of the signal at a given absorbed energy. They determine the relative resolution $\Delta E/E$. For semiconductors the signal fluctuations are smaller than the simple statistical variance $\sigma_Q = \sqrt{N_Q}$, where N_Q is the number of released charge pairs (ratio between the total deposited energy E_0 and the average energy deposition E_i required to produce an electron-hole pair). [] shows that the variance is $\sigma_Q = \sqrt{FN_Q}$, where F is the Fano factor [] (0.08 for diamond and 0.115 for silicon []). Thus, the variance of the signal charge is smaller than expected, $\sigma_Q \approx 0.3\sqrt{N_Q}$. The resulting intrinsic resolution of semiconductor detectors is

$$\Delta E_{FWHM} = 2.35\sqrt{FEE_i} \quad (1.10)$$

wherein $E_i(Si) = 3.6$ eV and $E_i(C) = 13$ eV. E.g., for an α particle with energy $E_\alpha = 5.486$ MeV the calculated resolution in diamond is equal to $\Delta E_{FWHM} = 5.6$ keV. This defines the maximum achievable resolution for energy spectroscopy with semiconductors. Figure ?? shows the calculated energy resolution function for silicon and diamond.

1.2 Carrier transport in a diamond sensor

This section describes the carrier transport phenomena in diamond. This theory provides the basis for discussion about the measurements in chapter ??.

Free charge carriers in a semiconductor get thermally excited and scatter in random directions with a thermal velocity v_{th} []. Their integral movement due to thermal

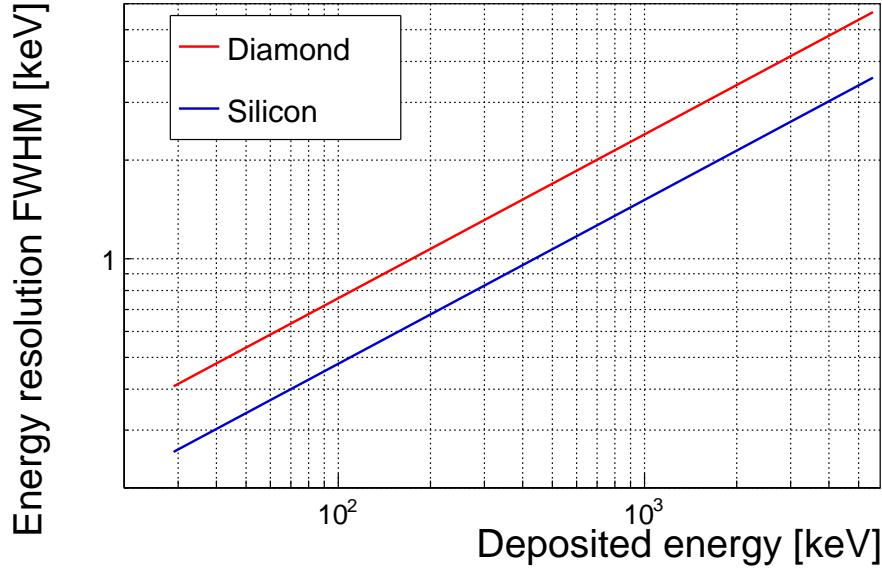


Figure 1.5: Calculated intrinsic energy resolution for silicon and diamond.

162 excitation equals zero. Their transport is instead by means of drift and diffusion. Dif-
 163 fusion is caused by the concentration gradient. In its presence the carriers tend to
 164 scatter in the direction of the lower concentration. Drift on the other hand is caused
 165 by an externally applied electrical field. In that case the carriers move in parallel to
 166 to the field lines. In a sensor with a high applied field the diffusion contribution is
 167 negligible.

168 **Diffusion** The concentration profile dissolves with time forming a Gaussian distri-
 169 bution with variance $\sigma(t) = \sqrt{Dt}$ [] .

170 **Drift velocity and mobility** The charge carriers drift through the diamond bulk
 171 with a drift velocity $v_{\text{drift}}(E)$ [], which is proportional to the electric field E at low
 172 electric fields: $v_{\text{drift}} = \mu E$. The proportionality factor μ is defined as the mobility in
 173 $\text{cm}^2\text{V}^{-1}\text{s}^{-1}$. For higher fields, however, the velocity saturates. The final equation for
 174 v_{drift} is therefore

$$v_{\text{drift}}(E) = \mu(E)E = \frac{\mu_0 E}{1 + \frac{\mu_0 E}{v_{\text{sat}}}} \quad (1.11)$$

175 where μ_0 is the low field mobility and v_{sat} is saturation velocity. The drift velocity can
 176 be retrieved experimentally via the transit time measured with the Transient Current
 177 Technique (TCT). This technique enables the measurement of transit time t_t of the
 178 carriers through the sensor with the thickness d .

$$v_{\text{drift}}(E) = \frac{d}{t_t(E)}. \quad (1.12)$$

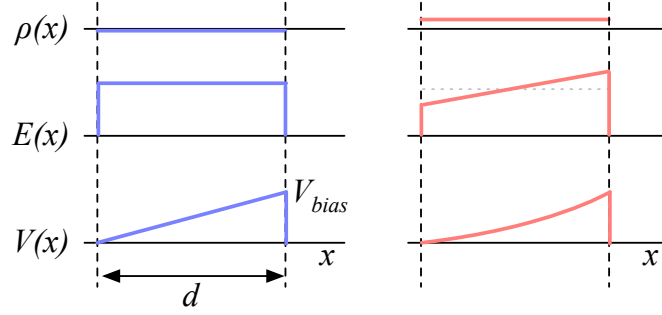


Figure 1.6: Introduction of space charge in the diamond bulk. The induced current signal is proportional to the effective electrical field. d is the thickness of the diamond sensor.

179 The velocities for holes and electrons usually differ. In diamond, the holes travel
 180 30 % faster than electrons []. The measurements in chapter ?? empirically confirm
 181 this statement.

182 **Velocity saturation** At higher drift velocities the carriers lose more energy to the
 183 lattice. They induce increasingly more lattice vibrations (phonon transport) with
 184 increased velocity. There is a velocity limit above which the carriers cannot reach –
 185 velocity saturation. Thesis [] defines this velocity to be $v_{\text{sat}}^e = v_{\text{sat}}^h = (14.23 \pm 0.12) \times$
 186 10^6 cm/s for both positive and negative charge carriers.

187 **Space charge** Poisson’s equation shows that

$$\frac{d^2\Phi(x)}{dx^2} = \frac{dE(x)}{dx} = \frac{\rho(x)}{\epsilon} \quad (1.13)$$

188 where $\rho(x)$ is the space charge distribution, E is the electrical field and Φ is the voltage
 189 potential. In an ideal diamond, the externally applied high voltage potential on the
 190 two electrodes decreases linearly through the bulk. The electrical field is therefore
 191 constant throughout the sensor and the space charge distribution across it equals
 192 0. However, in some cases space charge is introduced in the bulk, uniformly or non-
 193 uniformly. It can do so by means of trapping of charge carriers in the non-uniformities
 194 in the lattice or it can already be introduced during the production of the diamond
 195 material. The space charge can be either permanent or changing – sometimes it is
 196 possible to reduce it by means of priming. All in all, it is very important to reduce
 197 it because it affects the shape of the electrical signal. Since the drift velocity of
 198 the charge carriers is proportional to the electrical field, the charges change their
 199 velocity while drifting through the space charge region. Figure ?? compares the
 200 voltage potential, electrical field, space charge for an ideal sensor and for that with a
 201 uniformly distributed positive space charge.

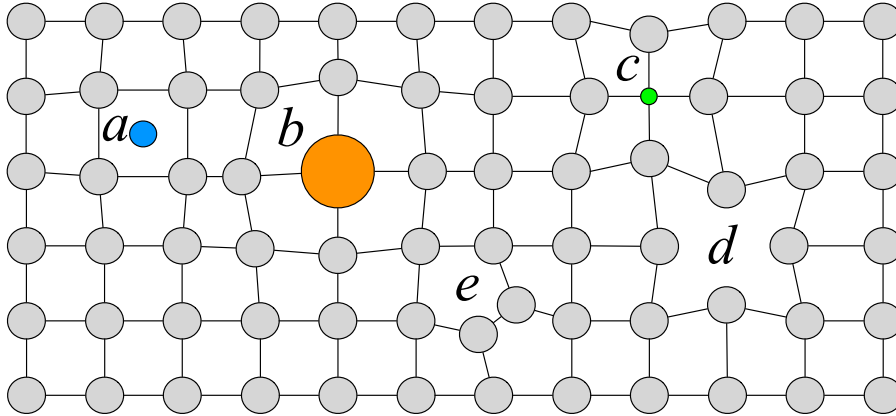


Figure 1.7: Introduction of impurities and non-uniformities into the crystal lattice due to radiation damage.

Radiation damage The diamond crystal lattice is very strong and uniform. However, when the highly energetic particles or photons impinge the diamond, they can damage the crystal structure. Figure ?? shows several examples of the lattice damage:

- a) foreign interstitial (e.g. H, Li),
- b, c) foreign substitutional (e.g. N, P, B),
- d) vacancy and
- e) self interstitial.

These non-uniformities – traps – form new energy levels in the forbidden gap. The drifting charge carriers are stopped by these traps, which in effect reduces the induced current. The energy level of the trapped carrier is reduced from the conduction band to the energy level of the trap. Different types of lattice damage have different energy levels. The release time depends on the level (shallow, deep trap).

1.3 Electronics for signal processing

This section describes the electronics of a detector, starting with a description of signal amplifiers and then discussing the digitisation and signal processing. All these stages are necessary to extract information from the sensor. First, the signal has to be amplified. Then it is digitised and finally processed in a specially designed processor or a logic unit.

1.3.1 Signal preamplifiers

The signal charge generated in the sensor by a single highly energetic particle or photon is of the order of fC. The induced current is ranging between 10^{-8} A (β, γ

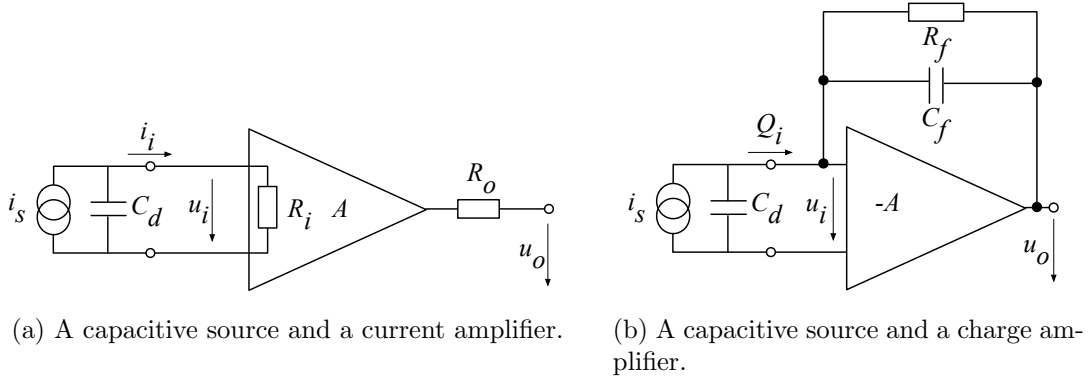


Figure 1.8: Simplified equivalent circuits of a current and charge amplifier.

223 radiation) and 3×10^{-7} A (α radiation). Signals as low as these have to be pre-
 224 amplified before processing. Depending on the measurement, several types of signal
 225 amplifiers can be used. The preamplifiers have to be designed carefully to minimise
 226 electronic noise while maximising gain – thus maximising the signal-to-noise ratio
 227 (SNR). In addition, they have to have a high bandwidth limit because the signals
 228 from the diamond sensors are very short. A critical parameter is the total capacitance,
 229 i.e. sensor capacitance and input capacitance of the preamplifier. The SNR improves
 230 with a lower capacitance. Several types of amplifiers can be used, all of which affect
 231 the measured pulse shape. They behave differently for resistive or capacitive sources.
 232 This thesis focuses on semiconductors as capacitive sources. Two preamplifiers are
 233 used most commonly, a current and a charge amplifier. Both are described below in
 234 detail.

235 Current-sensitive amplifier

236 Figure ?? shows the equivalent circuit of a capacitive source and a current ampli-
 237 fier. An amplifier operates in current mode if the source has a low charge collection
 238 time t_c with respect to the $R_i C_d$ time constant of the circuit. In this case the sensor
 239 capacitance discharges rapidly and the output current i_o is proportional to the in-
 240 stantaneous current i_i . The amplifier is providing a voltage gain, so the output signal
 241 voltage u_o is directly proportional to the input voltage u_i :

$$u_o(t) = A \cdot R_i \cdot i_s(t). \quad (1.14)$$

242 The detector capacitance C_{det} together with the input resistance of the amplifier R_i
 243 defines the time constant of the signal (see figure ??). The higher the C_{det} , the slower
 244 is the response of the amplifier. For the case of the diamond sensor, which has the
 245 capacitance of the order of 2 pF and the input resistance of 50 Ω , the resulting time
 246 constant is $\tau = 10^{-10}$ s. This yields the signal rise time $t_r \sim 2.2\tau = 0.22$ ns.

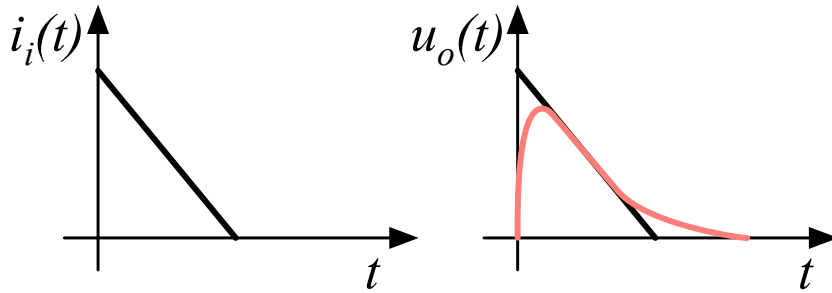


Figure 1.9: Input and output signal of the current amplifier.

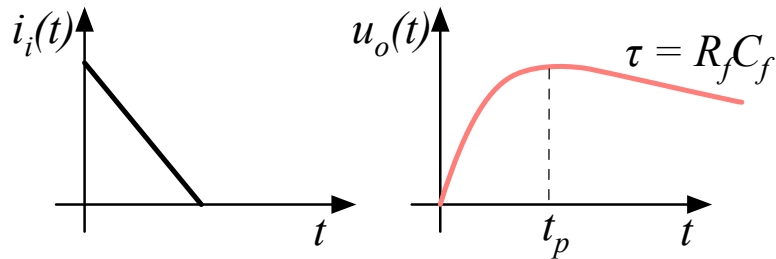


Figure 1.10: Input and output signal of the charge amplifier.

Charge-sensitive amplifier

In order to measure integrated charge in the sensor, a feedback loop is added to the amplifier (see figure ??). The feedback can be used to control the gain and input resistance, as well as to integrate the input signal. The charge amplifier is in principle an inverting voltage amplifier with a high input resistance.

In an ideal amplifier the output voltage u_o equals $-Au_i$. Therefore the voltage difference across the capacitor C_f is $u_f = (A + 1)u_i$ and the charge deposited on the capacitor is $Q_f = C_f u_f = C_f (A + 1)u_i$. Since no current can flow into the amplifier, all of the signal current must charge up the feedback capacitance, so $Q_f = Q_i$.

In reality, however, charge-sensitive amplifiers respond much slower than is the duration of the current pulse from the sensor. In addition, a resistor is added to the feedback line in parallel to the capacitor. The resistor and capacitor define the decay time constant of the pulse (see figure ??). This is necessary to return the signal to its initial state and ready for a new measurement.

Analogue electronic noise

Electronic noise determines the ability of a system to distinguish signal levels. The analogue signal contains a lot of information, which can quickly be erased or altered if the signal properties change. It is therefore instrumental to understand the noise contributions to the signal to qualify the information it carries. There are several noise contributions, of which the important ones are listed below. The thermal noise is the dominant noise contribution in the use case for diamond detector signal amplification and therefore defines the limitations of the detector system. Thermal noise or Johnson–Nyquist [] noise is generated by the random thermal motion of charge carriers in the conductor. The frequency range of the thermal noise is from 0 to ∞ with a more or less uniform distribution. Therefore this is nearly a white noise. The resulting signal amplitude has a Gaussian distribution. The RMS of the noise amplitude is defined as

$$u_{\text{RMS}} = \sqrt{4k_B R T \Delta f} \quad (1.15)$$

where k_B is the Boltzmann constant, R is the resistance of the conductor, T its temperature and Δf the frequency range. This equation shows that it is possible to reduce the noise RMS by either (1) reducing the frequency range, (2) reducing the resistance of the conductor or (3) cooling the conductor.

Contributions of shot noise, flicker noise and burst noise and other types are not significant relative to the thermal noise. However, the contributions of external factors can severely deteriorate the signal. This means the noise produced by capacitive or inductive coupling with an external source, which causes interference in the signal. These effects can be reduced by shielding the electronics and avoiding ground loops.

1.3.2 Analogue-to-digital converters

An analogue-to-digital converter (ADC) is a device that converts the analogue electrical signal on the input to its digital representation - a series of digital values. This involves a quantisation – *sampling* of the signal at a defined sampling period, resulting in a sequence of samples at a discrete time period and with discrete amplitude values. The resolution of the ADC is the number of output levels the ADC can quantise to and is expressed in bits. For instance, an ADC with a resolution equal to $n = 8$ bit has a dynamic range of $N = 2^n = 256$ steps. The resulting voltage resolution Q_{ADC} at the input voltage range of $V_{\text{ADC}} = \pm 50$ mV is then equal to

$$Q_{\text{ADC}} = \frac{V_{\text{ADC}}}{2^n} = \frac{100 \text{ mV}}{2^8 \text{ steps}} = 0.39 \text{ mV/step}. \quad (1.16)$$

With a sampling period of $t_s = 1$ ns the sampling rate is $f_s = 1$ GSPS (gigasample per second).

Quantisation error and quantisation noise (or a round-off error) is a contribution to the overall measurement error due to digitisation (rounding). It is defined as a difference between the actual analog value and a digitised representation of this

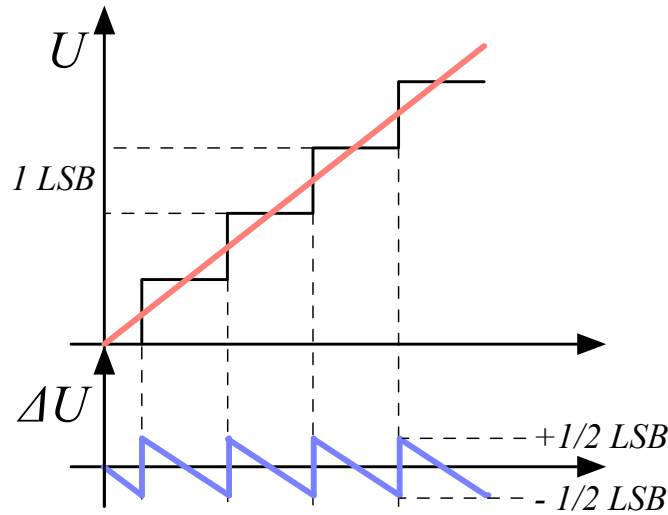


Figure 1.11: Input signal digitisation and quantisation error.

value. The error is defined by the least significant bit (LSB), as seen in figure ??.

Typically, the input signal amplitude is much larger than the voltage resolution. Therefore the quantisation error is not directly correlated with the signal and has an approximately uniform distribution []:

$$\Delta Q_{\text{ADC}} = \frac{1}{\sqrt{12}} \text{LSB} \sim 0.289 \text{ LSB}. \quad (1.17)$$

For the example above the quantisation error equals $\Delta Q_{\text{ADC}} = 0.289 \cdot 0.39 \text{ mV} = 0.11 \text{ mV}$.

The error depends strongly on the linearity of the ADC, but this is not discussed in this document as the devices used have ADCs with a linear response.

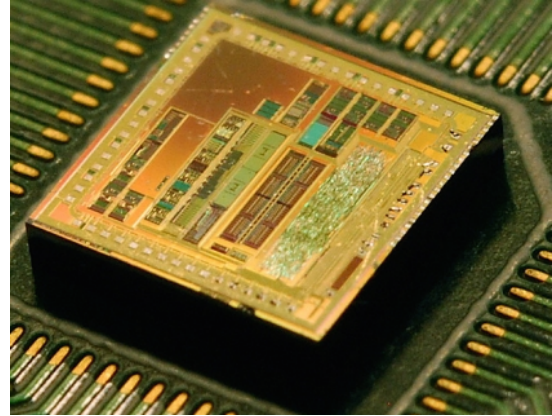
1.3.3 Digital signal processing

The digitised signal can be processed to extract useful information. Therefore after the signal amplification and digitisation the signal is routed in a device which handles the analysis. The signal can either be processed immediately (in real time) or it can be saved to a data storage for analysis at a later stage (offline). The devices carrying out the processing can be multipurpose (e.g. Field programmable gate arrays) or dedicated (e.g. application-specific integrated circuits). Each of the two has its advantages and disadvantages, which are listed below.

Field programmable gate array (FPGA) is an integrated circuit designed to be reprogrammable and reconfigured after manufacturing. It consists of a set of logic gates that can be interconnected in numerous combinations to carry out a logic operation. Many such logic operations can take place in parallel, making the FPGA a



(a) Xilinx Virtex 5 FPGA [?].



(b) ASIC [?].

Figure 1.12: An example of an FPGA and an ASIC chip.

powerful tool for signal processing. FPGAs are often used during system development or in systems in which the requirements might change with time. They can be reprogrammed in the order of seconds. In addition, the logic design only needs minor changes when migrating to a newer version of the FPGA chip of the same vendor. They also offer faster time-to-market with comparison to application-specific solutions, which have to be developed. On the other hand, the price per part can be significantly higher than for the application-specific solutions. Also, their other major disadvantages are a high power consumption and a relatively low speed. However, today's solutions are capable of clock speeds of the order of 500 MHz. Together with the integrated digital signal processing blocks, embedded processors and other modules, they are already very powerful and versatile. All in all, FPGAs are a good choice for prototyping and limited production, for projects with a limited requirements for speed and complexity.

Application-specific integrated circuit (ASIC) is an integrated circuit designed for a specific use. The design cannot be modified after chip production, as compared to FPGAs. On the other hand, the ASICs can be optimised to perform a required operation at a high speed and at a low power consumption. In addition, due to the specific design the size of the chip can be much smaller. ASICs can be designed as hybrid chips, containing both a digital and an analog part. To update the chip, the design has to be submitted to a foundry, which produces the new chips with a turnover time of 4—6 weeks. The costs of a submission start at \$ 50 000, but the price per part can be reduced significantly with a high volume. To sum up, ASICs are used for high volume designs with well defined requirements where some stringent constraints in terms of power consumption and speed have to be met.